Sensing Coastal Erosion

Jenna Schellekens

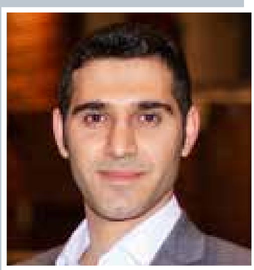

Dr. Meisam Amani

Schellekens and Amani use optical imagery to determine the magnitude of coastal erosion.

Who should read this paper?

This paper is of interest for those involved with remote sensing applications in marine/coastal science. The study explores the utilization of Landsat satellite imagery and machine algorithm to examine coastal erosion.

Why is it important?

The study utilizes an advanced remote sensing technology to analyze coastal erosion. The proposed method can be applied to various locations in a cost-effective and safer manner than field surveys. The results can be implemented for data collection and examination in various locations. The ocean community may benefit from the efficiency and cost-effectiveness of the machine algorithm and remote sensing applications.

About the authors

Jenna Schellekens is a 2021 graduate of the Diploma of Marine Environmental Technology program at the Fisheries and Marine Institute of Memorial University of Newfoundland. She is currently completing her bachelor of engineering/applied science.

Dr. Meisam Amani is the remote sensing team lead and the key specialty leader of data science at Wood PLC, a global consulting and engineering company, where he manages and leads various industrial, governmental, and academic remote sensing projects worldwide. Over the past 11 years, he has worked on different applications of remote sensing, including but not limited to land cover/land use classification, soil moisture estimation, drought monitoring, water quality assessment, watershed management, power/transmission line monitoring, fog detection and nowcasting, and ocean wind estimation. To do these, he has utilized various remote sensing datasets (e.g., UAV, optical, lidar, SAR, scatterometer, radiometer, and altimeter) along with different machine learning and big data processing algorithms. A list of his research works, including over 50 peer-reviewed journal and conference papers, can be found at www.researchgate.net/profile/Meisam_Amani3.

COASTAL EROSION DETECTION USING LANDSAT SATELLITE IMAGERY AND SUPPORT VECTOR MACHINE ALGORITHM

Jenna Schellekens[1] and Meisam Amani[2]

[1]*Marine Environmental Technology, Fisheries and Marine Institute of Memorial University of Newfoundland, St. John's, N.L., Canada*

[2]*Wood Environment & Infrastructure Solutions, Ottawa, O.N., Canada; meisam.amani@woodplc.com*

ABSTRACT

Erosion of coastal dunes and embankments has been an ongoing issue of the smallest Canadian province (i.e., P.E.I.) because it is largely composed of easily damaged sandstone. As more coast is eroded every year, more buildings, homes, environmental habitat, and provincial roads are at risk of being lost. This study is focused on the use of optical imagery acquired by Landsat-5 and Landsat-8, captured in September 1985 and June 2020, respectively, to determine the magnitude of coastal erosion on Robinson Island, P.E.I., Canada. The Support Vector Machine (SVM) algorithm, along with several ArcGIS software tools, were employed to map and interpret the erosion in this coastal area. The classification results, with Overall Accuracies (OA) of 97.86% and 98.46% respectively in 1985 and 2020, indicated that approximately 50.37% (i.e., from 1.35 km^2 to 0.68 km^2) coastal area was eroded. The results of this study are important to understand the magnitude of the erosion and adjust the required policies and mitigation actions for adaption to avoid possible environmental hazards.

KEYWORDS

Coastal erosion; Landsat; Remote sensing; Support Vector Machine (SVM); Machine learning

INTRODUCTION

Coastal zones are dynamic environments, which provide diverse ecosystem services, including storm buffering, pollution removal, and nutrient cycling [Ferreira et al., 2017]. These areas are continuously interacting with sea and ocean waters, and as a result, are prone to substantial land dynamics [Ahmed et al., 2018; Amani et al., 2021]. Additionally, the sea level rise and other catastrophic natural events (i.e., hurricanes, storms, and tsunamis) adversely affect these dynamic environments [Carrasco et al., 2016; Amani et al., 2021]. In fact, natural phenomena, climate change, alteration of sediment supplies, and anthropogenic activities resulted in severe coastal erosion and parallel accretion. This has drawn the attention of the scientific community and also policy-makers to extract reliable and instant information about the coastal area changes linked to erosion and accretion.

Field surveys and static ground stations provide the most accurate information to address coastal erosion/accretion [Ghosh et al., 2015]. However, these approaches are resource-intensive and also provide limited observation along the coast. Consequently, remote sensing data has been identified as a beneficial approach to study and monitor coastal variabilities [Ghosh et al., 2015; Amani et al., 2021]. Additionally, the availability of remote sensing historical data permits the quantification of coastal erosion/accretion through time. Meanwhile, machine learning (ML) algorithms and Geospatial Information System (GIS) software allow the extraction of concerned information from remote sensing data in a more automatic and sophisticated manner [Maxwell et al., 2018].

Many studies have been dedicated to investigating the coastal variability integrating different types of remote sensing datasets. For instance, Ahmed et al. [2018] employed two Landsat-5 images, acquired in 1985 and 1995, and two Landsat-7 images, acquired in 2005 and 2015, to measure the erosion and accretion of the entire coastal areas of Bangladesh. In this regard, through the investigation of the spectral responses, a thresholding analysis step was applied to the near infrared (NIR) band of each image to distinguish coastal areas from water, followed by manual digitization. Their results suggested that the study area experienced 1,576 km^2 and 1,813 km^2 erosion and accretion, respectively, leading to a final gain of 237 km^2. Moreover, Valderrama-Landeros and Flores-de-Santiago [2019] utilized air photos, Landsat, and SPOT-5 images to assess the coastal variations of San Pedro and Santiago along the Pacific coast of Mexico between 1970 and 2015. The extracted coastal boundaries, using thresholding and visual inspection steps, were injected into Digital Shoreline Analysis System [Thieler and Danforth, 1994] to determine the rate of changes. The results revealed a total of 6.69 km^2 erosion and 3.79 km^2 accretion in Santiago and San Pedro, respectively. Likewise, multispectral remote sensing data of Landsat-2, Landsat-5, Landsat-7, and Sentinel-2 were employed to assess the coastal erosion and accretion of Cua Dai estuary, Vietnam [Cham et al., 2020]. A hierarchical thresholding step was used to extract shoreline boundaries, followed by a tidal correction analysis using digital elevation model data. The trend analyses indicated average erosion/accretion rates of approximately 8.8/4.2 metres per year, resulting in a total loss of

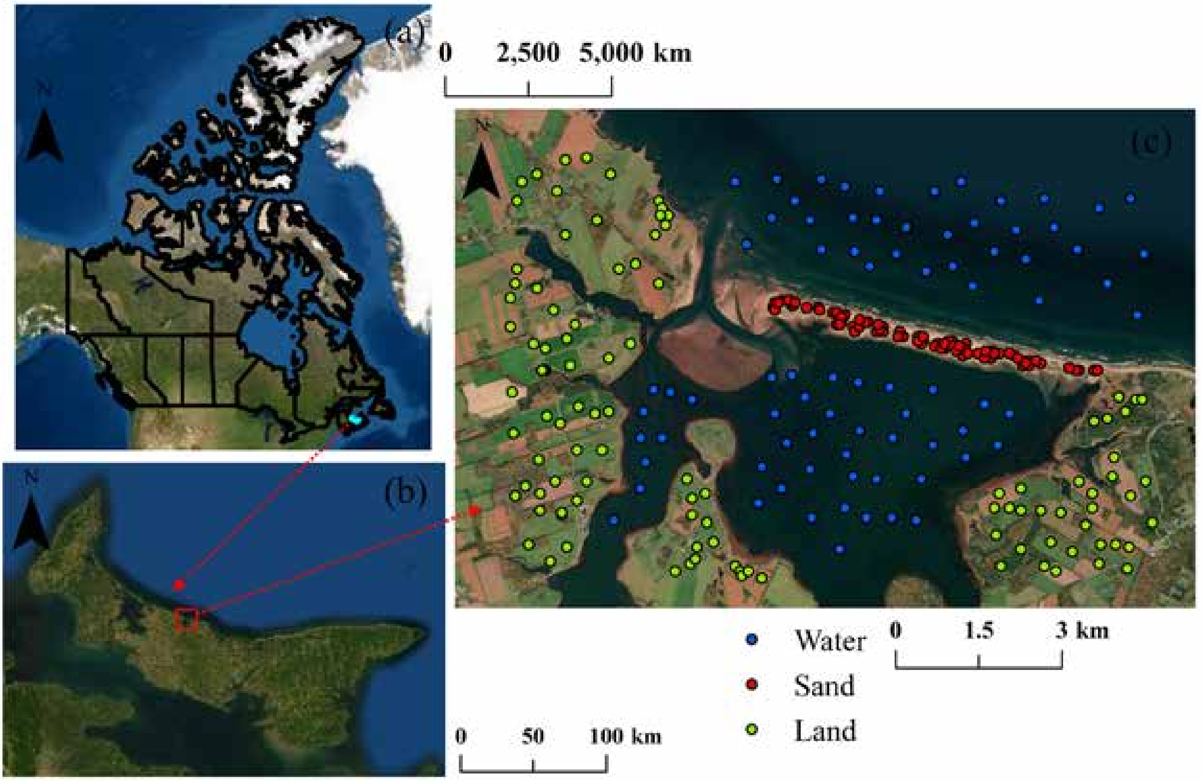

Figure 1: The geographical location of the study area, along with the distribution of the reference samples collected through precise visual interpretation of satellite images.

about 2.82 km^2 coastal area. Finally, Duru [2017] employed Landsat-7 and Landsat-8 images between 1975 and 2016 to measure the shoreline changes of Lake Sapanca, Turkey. In this regard, after several preprocessing steps, two spectral indices of the Normalized Difference Water Index (NDWI) and Modified NDWI were ingested into a maximum likelihood classifier to delineate the shoreline boundary. It was reported that the maximum erosion/accretion rates were 0.6/11.9 metres per year between 1975 and 2016.

Considering the long-term effect of different natural and anthropogenic phenomena on coastal dynamics, the objective of this study is to use ML techniques along with satellite imagery to assess the coastal erosion in Robinson Island and nearby areas in Prince Edward Island (P.E.I.). To this end, two Landsat-5 and Landsat-8 satellite imagery, respectively acquired in 1985 and 2020, were employed. Moreover, very high-resolution Google Earth imagery was used to assess the erosion zones visually.

STUDY AREA AND DATA

Study Area

The study area is Robinson Island and nearby areas in P.E.I., Canada. This area was selected because it is located along the north shore of P.E.I. and is open to the Atlantic Ocean wave action and heavy tourism during the summer. The area is also an important nesting ground habitat for seabirds, such as terns and the endangered piping plover. Figure 1 shows the geographical location of Robinson Island along with the reference samples. In this study, no in-situ data

Figure 2: (a) RGB colour composite of Landsat-5 image acquired in 1985 and (b) RGB colour composite image of Landsat-8 acquired in 2020.

was used. However, reference samples in three classes of Sand, Land, and Water were collected through precise visual interpretation of satellite images. For this, a false-colour composite of satellite imagery was used to distinguish suitable samples for each class. These reference samples were later used to train the ML algorithm and validate the results.

Satellite Data

Two Landsat-5 and Landsat-8 satellite images, respectively acquired on September 14, 1985, and June 10, 2020, were employed to analyze and quantify coastal erosion in the study area (Figure 2).

Landsat-5 was launched in 1984, orbiting the Earth in a sun-synchronous motion at the altitude of 705 km with a repeat cycle of 16 days and carried the multispectral scanner and the thematic mapper (TM) instruments. The TM data, which was in this study, were captured in seven spectral bands, including three visible, two NIR, one middle infrared, and one thermal. It is worth noting that only optical bands with a spatial resolution of 30 m were employed to delineate the coastal area in 1985.

Landsat-8 is the most recently launched satellite of the Landsat Data Continuity Mission (i.e., 2013) and carries the operational land imager (OLI) and the thermal infrared sensor (TIRS) instruments. Here, the optical data acquired by the OLI instrument in seven spectral bands (i.e., visible, NIR, and shortwave infrared) with a spatial resolution of 30 m were employed to extract the coastal area in 2020 for further processing.

METHODOLOGY

The implemented workflow includes three steps of (1) satellite data preprocessing, (2) coastal area delineation using SVM ML algorithm, and (3) manual refinements of the classification results and coastal erosion assessment, which are separately described below.

In the first step, after downloading the Landsat satellite images from https://earthexplorer.usgs.gov/, several preprocessing steps, including radiometric calibration (i.e., converting digital number values to the top of atmosphere radiances), atmospheric correction (i.e., reducing the atmospheric effects and converting radiances to the surface reflectance values), and masking of the study area, were applied to each satellite image for further processing. Second, the preprocessed images were injected into the SVM classifier with the linear kernel function to produce the classified maps. It should be mentioned that a linear kernel function was implemented since the considered classes (i.e., Sand, Land, and Water) were reasonably linearly separable using hyperplanes [Kavzoglu and Colkesen, 2009]. Meanwhile, the reference samples were randomly split into two independent groups of training (50%) and test (50%) samples. Training samples were used to train the SVM classifier, whereas the test samples were employed to statistically validate the classification results through computation of the confusion matrix and other accuracy metrics (i.e., Overall Accuracy (OA), Kappa Coefficient (KC), producer and user accuracies, commission and omission errors) to ensure their reliability [Foody, 2002]. Third, the classification maps were converted to polygon vectors, and manual refinements, especially in the coastal area, were performed to enhance the classification results. This step was applied to reduce possible errors in the classification results and making the results more accurate for further analysis. Finally, the boundaries of sandy coastal areas were extracted from both maps and were compared to evaluate the amount of erosion from 1985 to 2020.

RESULTS AND DISCUSSIONS

Figure 3 illustrates the two maps with three classes (i.e., Sand, Land, and Water) resulted from the SVM classifier. Visually, both maps are clear and provide satisfactory representations of the study area. Comparing

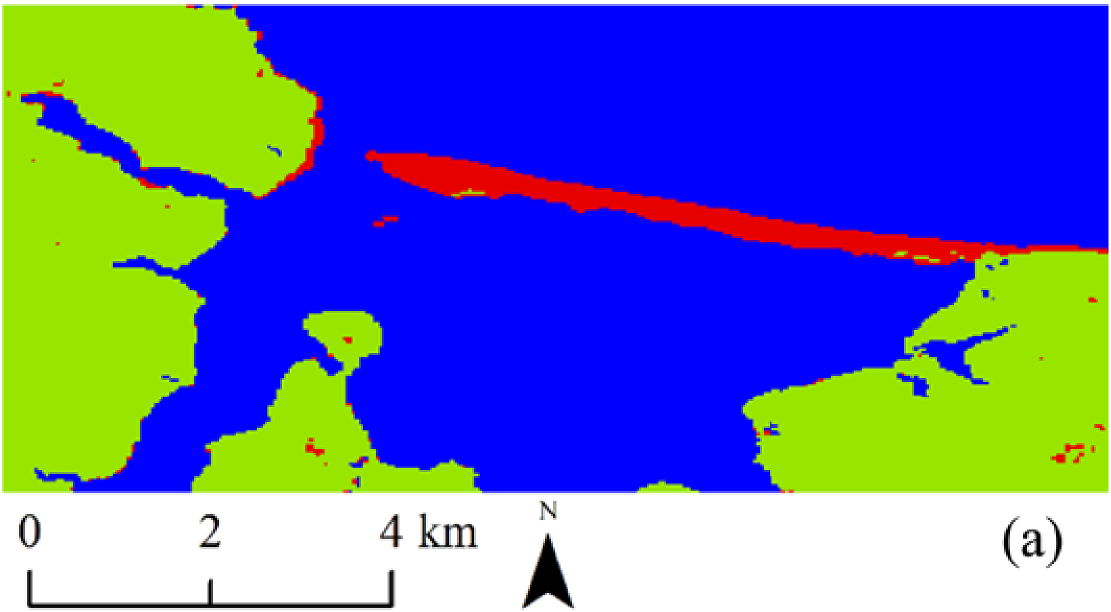

the classification results of 1985 (Figure 3 (a)) and 2020 (Figure 3 (b)), it is evident that the coastal area (i.e., Sand pixels among the Water) became shortened in length and smaller in area. Furthermore, to evaluate the reliability of the classification results using the SVM ML algorithm, test samples were employed to calculate the confusion matrices and the other derived validation criteria, where the results are provided in Tables 1 and 2. The validation step confirmed that both maps in 1985 and 2020 had high OAs of 97.86% and 98.46%, respectively. Moreover, the producer and user accuracies varied between 96% and 100%, suggesting the reliability of the classification results to provide a precise representation of the coastal change in Robinson Island.

As mentioned earlier, finally, the classification results were manually refined before coastal boundary extraction to decrease possible uncertainties associated with the classification step. Afterward, the enhanced classification results were converted into vector polygons, and the interested areas were delineated from both maps. The extracted boundaries of the coastal area (i.e., Sand regions in the classification map) of interest in both 1985 and 2020, superimposed on the Landsat-8 image, are shown in Figure 4. Based on the results, the areas of the coastal zones in 1985 and 2020 were approximately 1.35 km^2 and 0.68 km^2, respectively, indicating about 50.37% decline in coastal area. The extracted results suggest that the sandy coastal zone of Robinson Island was severely declined in the past 35 years. This may be rooted in the fact that this area is potentially vulnerable to erosion causes, such as wave action, wind, run-off, and human activity, which are out of the scope of this study.

This study only revealed the amount of change between 1985 and 2020, and further investigations are required to manifest the causes of such coastal decline. In fact, more analyses are necessary to determine whether this amount of decline in coastal area is entirely

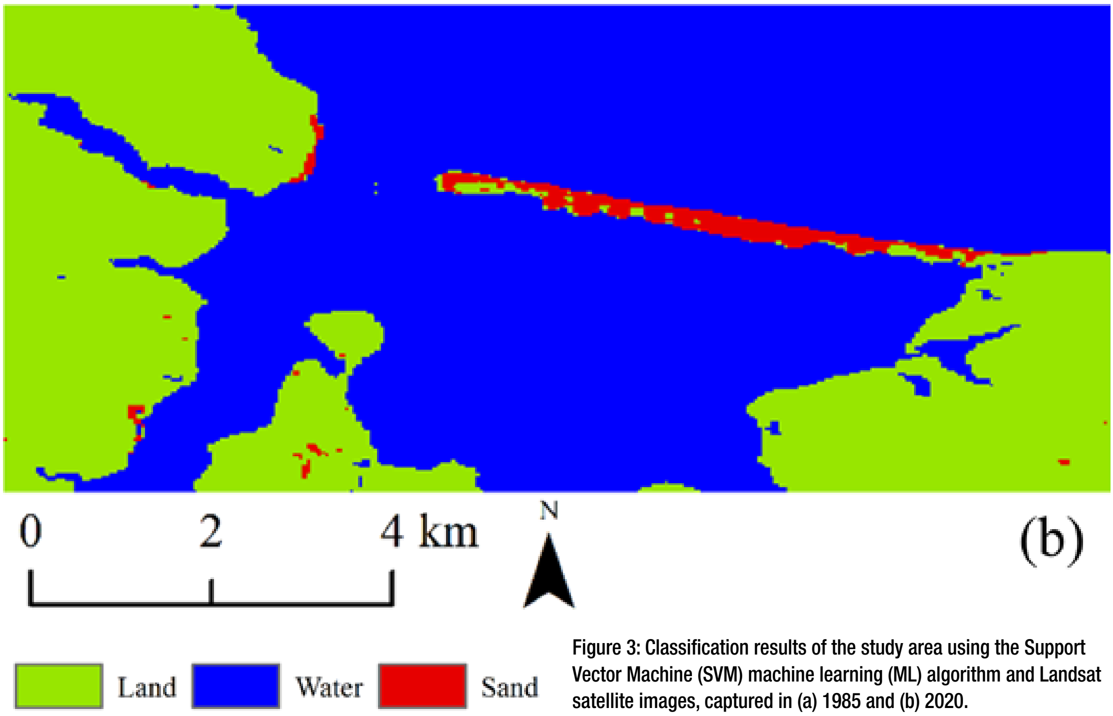

Figure 3: Classification results of the study area using the Support Vector Machine (SVM) machine learning (ML) algorithm and Landsat satellite images, captured in (a) 1985 and (b) 2020.

Table 1: The confusion matrix of the classified map in 1985 (Figure 3 (a)).

		Test Samples			Total	Commission Error (%)	User Accuracy (%)
		Sand	Land	Water			
Classified Data	Sand	96	2	0	98	2	98
	Land	4	98	0	102	4	96
	Water	0	0	100	100	0	100
	Total	100	100	100	300		
	Omission Error (%)	4	2	0		Overall Accuracy = 97.86%	
	Producer Accuracy (%)	96	98	100		Kappa Coefficient = 0.97	

Table 2: The confusion matrix of the classified map in 2020 (Figure 3 (b)).

		Test Samples			Total	Commission Error (%)	User Accuracy (%)
		Sand	Land	Water			
Classified Data	Sand	98	0	3	101	3	97
	Land	0	100	0	100	0	100
	Water	2	0	97	99	2	98
	Total	100	100	100	300		
	Omission Error (%)	2	0	3		Overall Accuracy = 98.46%	
	Producer Accuracy (%)	98	100	97		Kappa Coefficient = 0.98	

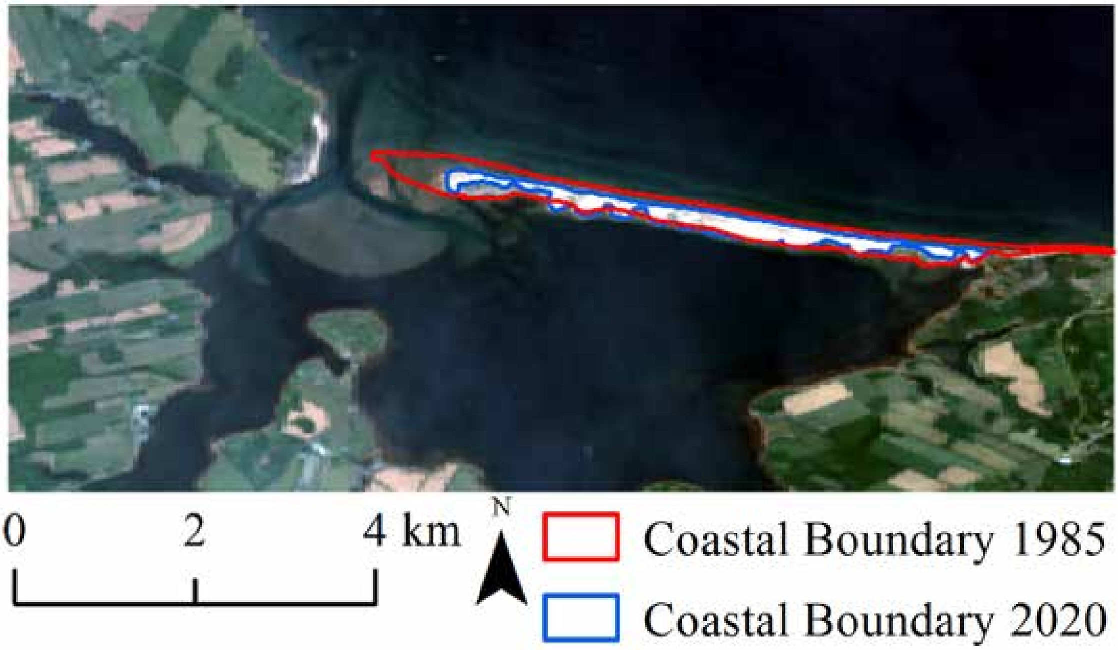

Figure 4: The boundary of coastal sand areas that was extracted based on the maps from Landsat imagery in 1985 and 2020.

associated with coastal erosion due to natural processes or anthropogenic activities, such as sand mining or drainage, in the last 35 years. For instance, Mujabar and Chandrasekar [2013] employed six different geospatial data for coastal area monitoring and reported a complex interaction of human-induced (e.g., manipulation of hydrological cycles, sand mining, and facility construction) and natural processes (e.g., sea level alterations, waves and current, and tectonics and storms events) as the reasons of coastal erosion. Additionally, in this study, the overall erosion was only investigated using two images acquired in 1985 and 2020 and, therefore, the rate of the change was not reported. Future studies should use a time-series of satellite images (e.g., one image per year) to investigate the erosion rate in more detail.

The implemented method has the advantage of the utilization of open access satellite imagery. The satellites easily collect data from all over the globe regularly and, due to their simplicity of processing, have attracted many scholars. The results of such studies are of significant importance to other coastal-related disciplines, including coastal management and conservation [Cruz-García et al., 2015], coastal vulnerability [Tahri et al., 2017], and sea level rise investigations [Dean and Houston, 2016]. The implemented approach can be employed along with other geospatial data, such as geomorphology, coastal slope, sea level variations, wave intensity variation, and anthropogenic footprints, to provide a comprehensive overview of the change of coastal area and to allow the determination of most contributing factors of erosion.

Like any other research study, this study includes several limitations, which can be further enhanced in future studies. The lack of collecting reference samples for classification through field surveys, especially in recent years (i.e., 2020), was a limiting factor that could slightly increase the uncertainties of the classification step. However, it should be noted that the precise visual interpretation of satellite images for reference samples collection, as well as the use of the SVM ML algorithm, resulted in accurate maps. Additionally, the very high-resolution satellite images in Google Earth were used to visually assess the results. However, the possibility of conducting field surveys to measure the sandy coastal area would definitely increase the robustness of the validation step.

To extend the obtained results and achieve comprehensive information about the erosion rate in P.E.I., it is recommended to consider other locations around P.E.I. for further investigations. Moreover, annual time-series Landsat imagery available from 1985 to the present along with other resources can be employed to quantify the rate of erosion of coastal areas in Robinson Island. In this case, the annual rate allows better monitoring of the amount of erosion and also can possibly provide the required information to investigate the causing of coastal erosion.

CONCLUSION

This study investigated the coastal erosion of Robinson Island in P.E.I., Canada. In this regard, the two Landsat satellite images in 1985 and 2020 were employed to quantify the amount of erosion. The SVM ML algorithm was used to classify the study area, and further post-processing steps were applied to enhance the classification results and to extract the coastline boundaries. The results revealed that the coastal area of interest experienced 0.67 km^2 erosion from 1985 to 2020. The use of free optical satellite data allows determining the coastal erosion in other parts of P.E.I. in a cost-effective manner. This can increase the understanding of coastal variation throughout P.E.I., and the achieved information will elucidate the operational path for other users and policy-makers for coastal management.

REFERENCES

Ahmed, A.; Drake, F.; Nawaz, R.; and Woulds, C. [2018]. *Where is the coast? Monitoring coastal land dynamics in Bangladesh: an integrated management approach using GIS and remote sensing techniques*. Ocean and Coastal Management, 151, 10-24.

Amani, M.; Ghorbanian, A.; Asgarimehr, M.; Yekkehkhany, B.; Moghimi, A.; Jin, S.; Naboureh, A.; Mohseni, F.; Mahdavi, S.; and Layegh, N.F. [2021]. *Remote sensing systems for ocean: a review (Part 1: Passive Systems)*. IEEE Journal of Selected Topics in Applied Earth Observations and Remote Sensing, Vol. 15, pp. 210-234, 2022, doi: 10.1109/JSTARS.2021.3130789.

Carrasco, A.R.; Ferreira, Ó.; and Roelvink, D. [2016]. *Coastal lagoons and rising sea level: a review*. Earth-Science Reviews, 154, 356-368.

Cham, D.D.; Son, N.T.; Minh, N.Q.; Thanh, N.T.; and Dung, T.T. [2020]. *An analysis of shoreline changes using combined multitemporal remote sensing and digital evaluation model*. Civil Engineering Journal, 6, 1-10.

Cruz-García, L.M.; Arreola-Lizárraga, J.A.; Ceseña-Beltrán, G.E.; Mendoza-Salgado, R.A.; Galina-Tessaro, P.; Beltrán-Morales, L.F.; and Ortega-Rubio, A. [2015]. *An examination of coastal conservation by remote sensing in Baja California Sur, México*. Journal of Coastal Conservation, 19, 609-619.

Dean, R.G. and Houston, J.R. [2016]. *Determining shoreline response to sea level rise*. Coastal Engineering, 114, 1-8.

Duru, U. [2017]. *Shoreline change assessment using multi-temporal satellite images: a case study of Lake Sapanca, NW Turkey*. Environmental

Monitoring Assessment, 189, 1-14.
Ferreira, Ó.; Plomaritis, T.A.; and Costas, S. [2017]. *Process-based indicators to assess storm induced coastal hazards*. Earth-Science Reviews, 173, 159-167.
Foody, G.M. [2002]. *Status of land cover classification accuracy assessment*. Remote Sensing of Environment, 80, 185-201.
Ghosh, M.K.; Kumar, L.; and Roy, C. [2015]. *Monitoring the coastline change of Hatiya Island in Bangladesh using remote sensing techniques*. ISPRS Journal of Photogrammetry and Remote Sensing, 101, 137-144.
Kavzoglu, T. and Colkesen, I. [2009]. *A kernel functions analysis for support vector machines for land cover classification*. International Journal of Applied Earth Observation and Geoinformation, 11, 352-359.
Maxwell, A.E.; Warner, T.A.; and Fang, F. [2018]. *Implementation of machine-learning classification in remote sensing: an applied review*. International Journal of Remote Sensing, 39, 2784-2817.
Mujabar, P.S. and Chandrasekar, N. [2013]. *Coastal erosion hazard and vulnerability assessment for southern coastal Tamil Nadu of India by using remote sensing and GIS*. Natural Hazards, 69, 1295-1314.
Tahri, M.; Maanan, M.; Maanan, M.; Bouksim, H.; and Hakdaoui, M. [2017]. *Using fuzzy analytic hierarchy process multi-criteria and automatic computation to analyse coastal vulnerability*. Progress in Physical Geography, 41, 268-285.
Thieler, E.R. and Danforth, W.W. [1994]. *Historical shoreline mapping (II): application of the digital shoreline mapping and analysis systems (DSMS/DSAS) to shoreline change mapping in Puerto Rico*. Journal of Coastal Research, 600-620.
Valderrama-Landeros, L. and Flores-de-Santiago, F. [2019]. *Assessing coastal erosion and accretion trends along two contrasting subtropical rivers based on remote sensing data*. Ocean and Coastal Management, 169, 58-67.